World Academy of Science, Engineering and Technology
International Journal of Energy and Power Engineering
Vol:8, No:11, 2014

MPC of Single Phase Inverter for PV System

Irtaza M. Syed, Kaamran Raahemifar

***Abstract*—**This paper presents a model predictive control (MPC) of a utility interactive (UI) single phase inverter (SPI) for a photovoltaic (PV) system at residential/distribution level. The proposed model uses single-phase phase locked loop (PLL) to synchronize SPI with the grid and performs MPC control in a dq reference frame. SPI model consists of boost converter (BC), maximum power point tracking (MPPT) control, and a full bridge (FB) voltage source inverter (VSI). No PI regulators to tune and carrier and modulating waves are required to produce switching sequence. Instead, the operational model of VSI is used to synthesize sinusoidal current and track the reference. Model is validated using a three kW PV system at the input of UI-SPI in Matlab/Simulink. Implementation and results demonstrate simplicity and accuracy, as well as reliability of the model.

***Keywords*—**Matlab/Simulink, Model Predictive Control, Phase Locked Loop, Single Phase Inverter, Voltage Source Inverter.

I. Introduction

RENEWED interest in single phase inverter (SPI) design and control is seen due to the renewable energy systems integration at distribution level [1]-[3]. Photovoltaic (PV) and wind has seen tremendous growth worldwide [4], [5]. Ease of installation, no moving parts, little to no maintenance requirement, and the non-stop decline in cost will continue to pave the road for application of PV at the distribution/residential level. This will result in a steady state market for the SPI on a global scale. SPI is either configured with the DC PV modules in the field or comes integrated with the DC PV modules as a micro-inverter. Micro-inverters on module level have less than or equal to 300W power [6], [7]. On the other hand, PV SPI for residential use can have a power ranging from few hundred watts to tens of kilowatts [8], [9]. In general, PV SPI comes with DC-DC converter (normally, a version of Boost), maximum power point tracking (MPPT) control and voltage source inverter (VSI) packed as a single unit. Sine or space vector pulse width modulation (SPWM and SVPWM) with a phase looked loop (PLL) and MPPT is the usual choice of control to synthesize in phase sinusoidal AC current and voltage at the connecting power utility frequency with maximum power and efficiency.

Literature review suggests multitude of controls based on repetitive [10], [11], dead-beat [12], [13], discrete-time sliding-mode [14], [15], synchronous reference frame (SRF) [3], and model predictive [16] control of SPI. Xue et al. [17] reviewed SPI for small distributed power generators, while Kjaer and colleagues [18] reviewed SPIs for PV.

As pointed out by Monfared et al. [3], repetitive control [10], [11] has excellent ability to eliminate periodic disturbances; however, it suffers from poor tracking accuracy, large memory requirement, in addition to poor non-periodic disturbances rejection ability. Complexity and sensitivity to parameter variations and loading conditions are the main problems with deadbeat [12], [13] and sliding-mode [14], [15] controllers, in spite of excellent dynamic performance in control of the instantaneous inverter output voltage. The SRF control [3], allows use of a conventional PI regulator that requires regulator adjustments, two orthogonal signals and has poor disturbance rejection capability due to the limited gain of PI regulators. Model predictive control (MPC) for utility interactive seven-level single phase inverter for system application is also reported in [16] with a focus of total harmonic distortion (THD and phase reduction through multiple levels and MPC.

Feedback controllers sense/measure a phenomenon to be controlled and feed errors/deviations back, if any, to the controller to process and adjust the controllable parameters in order to fix the error. In other words, the corrective action is taken after the error has occurred. On the other side, in MPC predictive control allows construction of controllers that can predict and fix errors before they actually occur. This predictive capability when combined with the feedback, results in a smoother control with optimal results better than feedback control alone. In the past, the MPC has been applied for industrial control, and recently it has been applied to the control of power converters due to its ease of implementation, constraints inclusion, inherent feedback and predictive control. The MPC considers a model of the system in order to predict the future behavior of the system over time [19], [20]. Appropriate switching state is selected based on a criterion defined by an objective function which represents the desired behavior of the system.

This paper presents a simple and easy to implement approach of modeling MPC based UI-SPI for PV systems. The paper is organized into seven sections: (I) Introduction, (II) SPI, (III) MPC, (IV) System Modeling and Control, (V) Simulation Results, and (VI) Conclusion.

II. Single Phase Inverter

SPI for PV systems usually consists of a DC-DC converter, maximum power point tracking (MPPT) control, PLL, VSI, and a control (Fig. 1) to synthesize AC current/voltage in synchronism with and at the grid frequency and voltage.

Irtaza M. Syed is a student at the Electrical & Computer Engineering Department, Ryerson University, Toronto, ON M5K 2K3 Canada (corresponding author phone: 647-787-6262; e-mail: i5syed@ ryerson.ca).

Dr. Kaamran Raahemifar, is with the Electrical & Computer Engineering Department, Ryerson University, Toronto, ON M5K 2K3 Canada, (e-mail: kraahemi@ee.ryerson.ca).

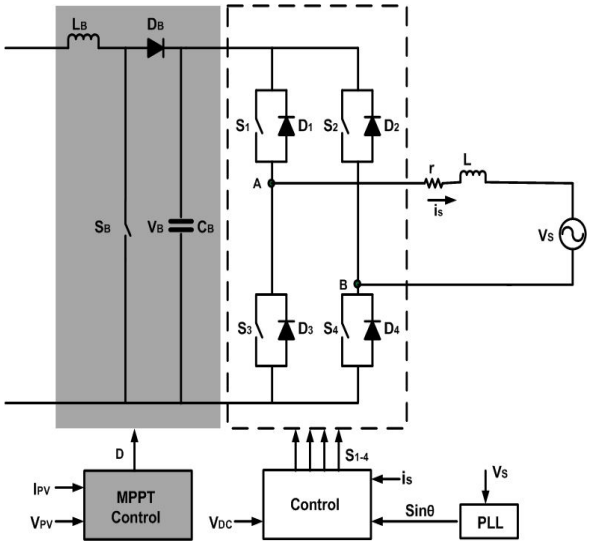

Fig. 1 SPI

A. Boost Converter

Output of the PV array varies due to variations in irradiance (G) and/or temperature (T). However, VSI requires stiff DC voltage equal to or greater than √2Vs at the input for satisfactory operation (1). Therefore, a DC-DC converter (Boost Converter, the shaded area in Fig. 1) is required to ensure the required fixed voltage. The output voltage of Boost Converter (BC) is calculated given by (2). D is the duty cycle, given by (3), and can assume any value between 0 and 1. Capacitor C (4) is selected according to the required amount of output voltage ripple. BC is operated in CCM mode, by choosing an L greater than L_{min} (to ensure I_L greater than I_{LB}) (5).

$$V_{DC} \geq \sqrt{2}V_i \quad (1)$$

$$V_O = \frac{1}{1-D}V_i \quad (2)$$

$$D = \frac{t_{on}}{T} \quad (3)$$

$$C_O = \frac{I_O}{\Delta V_O}DT \quad (4)$$

$$L \geq L_{min} = \frac{T}{2I_{LB}}D(1-D)V_O \quad (5)$$

B. MPPT Control

The maximum power point (P_{mp}), a point of operation for a PV array with maximum voltage (V_{mp}) and maximum current (I_{mp}), is ensured using the algorithm shown in Fig. 2. Perturb and Observe (P&O) MPPT control algorithm continuously adjusts PV array voltage and current based on the operating conditions, i.e., irradiation and temperature, to ensure P_{mp}. P&O MPPT algorithm (Fig. 2) is iterative. The maximum power point of operation is defined as follows:

1. Operating point is perturbed (present V_k & I_k measured)
2. Present P calculated ($P_k = V_k I_k$)
3. P_k is compared with $P_{(k-1)}$
4. Next perturbation direction is defined based on P_k & $P_{(k-1)}$

The process mimics the hill-climbing phenomenon to reach the peak of the mountain (maximum power point with V_{mp} & I_{mp}). This is to ensure the PV array operates at P_{mp}

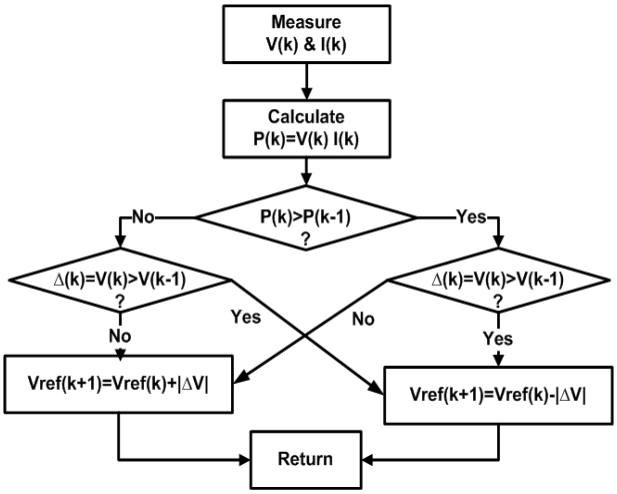

Fig. 2 P&O MPPT algorithm

C. Phase Locked Loop

In an AC power system, synchronization is the process of matching the frequency (or speed) of a VSI (or generator) with that of the connecting larger grid for power delivery into the grid. Phase-Locked Loop (PLL), a closed loop frequency control system, is used to synchronize SPI and the grid. Park's/Clark's transformations are not readily applicable for SPI synchronization of single phase systems since only a single phase is available in such systems. Therefore, a second orthogonal phase is created by delaying the single phase, Vs, by 90° (or T/4 cycle) Fig. 3. The *αβ* (Vs and 90° delayed Vs), still AC in nature, are converted into DC quantities *dq* to allow use of PI regulator. The voltage V_d is terminated (not used) and V_q is regulated to zero by a PI controller. Angular velocity, ω, is integrated to obtain theta, θ. θ is reset every cycle (or 2π) by Mod(2π) to start a new cycle in synchronism with the grid.

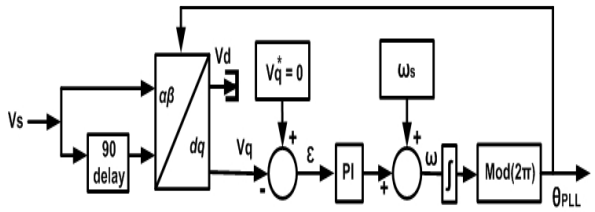

Fig. 3 PLL

D. Voltage Source Inverter

Full Bridge (FB) -VSI has four switches $S_{1\text{-}4}$ and is used to convert DC power into AC power at desired voltage and frequency. The switches are used to adjust the output voltage and frequency, in this case to equalize them with the grid voltage and frequency. Anti-parallel diodes are connected across the switches to allow reverse current flow. VSI requires a stiff DC voltage source at input for quality operation, supplied by DC-PV, a rectifier, battery, etc.

Fig. 4 shows a FB-VSI circuit connected to grid through resistor (R) and inductor (L) with a large capacitor (C_{DC}) to keep V_{DC} constant. VSI has two legs each with two switches

and two anti-parallel diodes each. Leg1, including S1, S3, D1 and D3 (a.k.a Half-Bridge Inverter (HBI)) is the basic building block of this type of inverters. FB-VSI has two HBIs in parallel. To avoid short circuit and for the bridge to operate properly, no two switches of the same HBI should be turned on simultaneously. By turning on the proper combination of switches, the output voltage, V_{AB} (or V_t) changes between $+V_{DC}$ and $-V_{DC}$, in addition to zero volts.

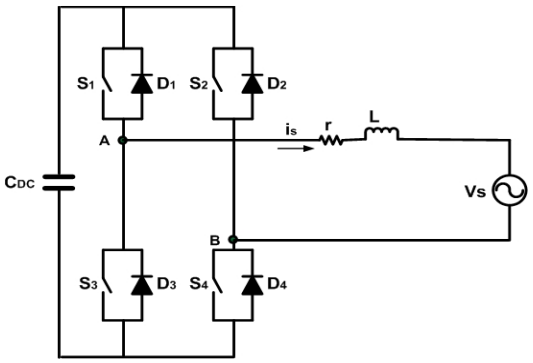

Fig. 4 FB-SPI Circuit

Output voltage is given by (6), with V_A and V_B given by (7) and (8).

$$V_O = V_A - V_B \quad (6)$$

$$V_A = (\frac{t_{on}}{T})V_{DC} \quad (7)$$

$$V_B = (\frac{t_{off}}{T})V_{DC} \quad (8)$$

If, duty cycle, D is given by (9) and switch turn off duration, t_{off} by (10) then Vo can be shown by (11). Equation (11) shows that the amplitude of VSI output can be adjusted by varying D.

$$D = \frac{t_{on}}{T} \quad (9)$$

$$t_{off} = T - t_{on} \quad (10)$$

$$V_O = (2D - 1)V_{DC} \quad (11)$$

E. Control

Conventionally, DC input voltage (V_{DC}) supplied by BC at the input of VSI is measured and compared against the reference voltage given by (1) (Fig. 5). The produced voltage error (V_E) is applied across PI or lead-lag voltage-control compensator for processing. The output of the compensator (I_D) is DC in nature and is multiplied by √2 and Sinθ to obtain the peak sinusoidal reference current (I_D^* equal to I_{DP}Sinθ) synchronized with the grid voltage V_s. The sinusoidal reference current is compared against the measured sinusoidal current (i_s) and the error is applied across current-control compensator to track the reference current with zero or minimal error. The output of the current-control compensator is applied across PWM controller to produce the appropriate switching sequence for the FB-VSI switches. PWM controller simply compares the output of the current-control compensator with triangular carrier wave to produce the switching sequence.

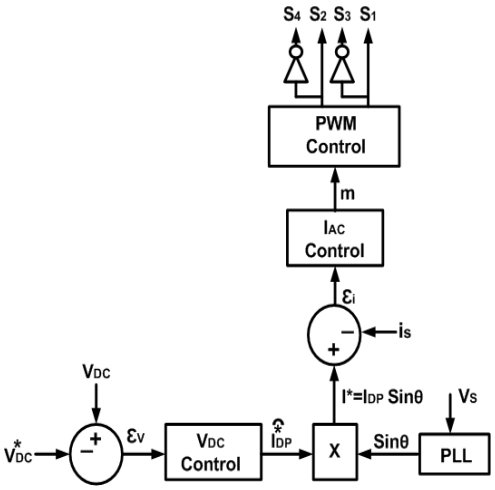

Fig. 5 Control

III. Model Predictive Control

The model predictive control strategy takes advantage of the fact that only a finite number of possible switching states are associated with SPI-VSI. These states are discrete and the model of the system can be used in association with a discrete-time model of the load to predict the behavior of the VSI system over a prediction horizon in time. MPC predictive control is used to predict and fix errors before they occur based on the desired behavior of the system; an objective function is defined for selection of the optimal future variables corresponding to the optimal future switching state. The objective of the MPC scheme is to predict the switching state and thus the current that tracks the reference/desired current with minimal error. For each sampling period, the resulted (predicted) output current is measured and compared with the reference current to minimize error. Usually the sampling period is selected in a way that it does not allow the reference current to change significantly during that period. The MPC algorithm for converters works as follows:

1. Appropriate/required initialization is done
2. Process model is defined (VSI operational model)
3. Control actions set is formed (00, 01, 10, 11)
4. The desired status for t=k+1 is defined (V_{k+1*}, I_{k+1*}, etc)
5. The system's present status is observed (V_k, I_k, etc)
6. Outputs for switching states (00 to 11) are determined
7. Outputs are compared with the desired output
8. Least error output =desired-measured → 0, selected
9. Corresponding switching state is determined
10. Corresponding switching state is applied at t=k+1
11. Output is observed and the process is repeated

These steps are summarized in Fig. 6.

As noted in step 6, the outputs for different control inputs are determined before the application of actual control switching states. Based on the process model (step 2), only the optimal switching state from the control action set (step 3) is applied to obtain the optimal output with the least possible error. In other words, outputs are estimated/predicted based on the present measurements/observations coupled with different input control actions. The optimal predicted output is selected

before any control action is applied. Thus, the optimal output with minimum or no error at all is selected. The system has inherent feedback mechanism (step 11), where output is observed and the process is repeated to choose another optimal switching state for the next t

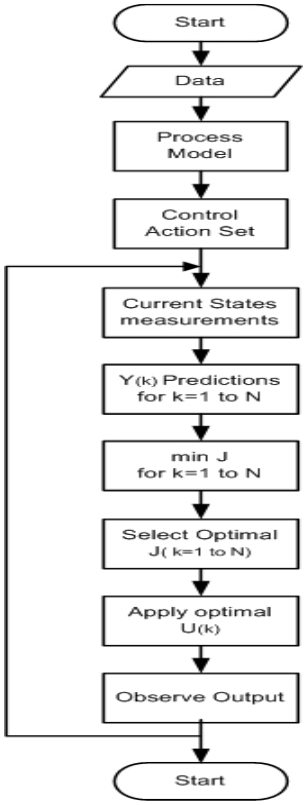

Fig. 6 MPC algorithm

IV. System Modeling And Control

The system modeling and control strategy followed in this paper is summarized as follows:

1. Model of the SPI converter is built
2. All possible switching states are determined
3. Model of the load is built for prediction
4. Objective function is defined

As discussed earlier, FB-VSI (Fig. 4) operation can be summarized as:

$$S_A = \begin{cases} V_{DC} \text{ if } S_1 \text{on and } S_3 \text{off} \\ 0 \quad \text{if } S_1 \text{off and } S_3 \text{on} \end{cases} \tag{12}$$

$$S_B = \begin{cases} V_{DC} \text{ if } S_2 \text{on and } S_4 \text{off} \\ 0 \quad \text{if } S_2 \text{off and } S_4 \text{on} \end{cases} \tag{13}$$

Then output voltage is:

$$V_O = (S_A - S_B)V_{DC} \tag{14}$$

where $S_A+S_B=1$ at any time.

Equation (14) is used to model FB-VSI to exercise SPI control in MPC.

Equations (12) and (13) or (14) also indicate that FB-VSI has 4 possible switching states with 2 active vectors and 2 zero vectors. The active vectors produce $+V_{DC}$ and $-V_{DC}$ while the zero vectors produce no output voltage (Table I).

TABLE I
SPI Active and Zero Vectors

Upper		Lower		Voltage	
S_1	S_2	S_3	S_4	V_t	Vector
0	0	1	1	0	$\mathbf{V_0}$
0	1	1	0	$+V_{DC}$	V_1
1	0	0	1	$-V_{DC}$	V_2
1	1	0	0	0	V_3

In addition< load dynamics are modeled as:

$$v = L\frac{di_s}{dt} + ri_s \tag{15}$$

where r and L are grid resistance and inductance, i_s is the current, and v is the VSI generated voltage vector. Using Euler-Forward Equation, the current i_s is approximated as:

$$\frac{di_s}{dt} \cong \frac{i_s(k+1)-i_s(k)}{T} \tag{16}$$

Combining (15) and (16) gives the following:

$$i_s^p(k+1) = \left(1 - \frac{rT}{L}\right) i_s(k) + \frac{T}{L} v(k) \tag{17}$$

where k is the present interval and k+1 is the upcoming interval for which the prediction is made. To exercise MPC in *dq* reference frame, the load current predicted in (17) can be expressed in the *dq* reference frame as:

$$\begin{bmatrix} i_{d(k+1)} \\ i_{q(k+1)} \end{bmatrix} = \begin{bmatrix} 1 - \frac{RT}{L} & 0 \\ 0 & 1 - \frac{RT}{L} \end{bmatrix} \begin{bmatrix} i_{d(k)} \\ i_{q(k)} \end{bmatrix} + \begin{bmatrix} \frac{T}{L} & 0 \\ 0 & \frac{T}{L} \end{bmatrix} \begin{bmatrix} v_{d(k)} \\ v_{q(k)} \end{bmatrix} \tag{18}$$

Equation (18) is used to predict the load current for each switching state. The objective function is evaluated for each of the 4 possible voltage vectors generated by the VSI to calculate the future optimal value of the load current. The optimal value of the objective function is applied during the next sampling period. Fig. 7 shows the VSI MPC control system.

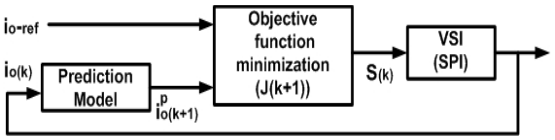

Fig. 7 SPI-VSI MPC control block diagram

Objective function J (19) is used to minimize the error ($r_{(k)}$) between the predicted output ($Y_{(k)}$) and measured reference ($i_{o\text{-}ref}$). The optimal $J_{(k+1)}$ with minimum error between the predicted and measured currents is selected and the corresponding control action ($U_{(k)}$) from control actions set, U = [00 01 10 11], is applied across VSI in the next sampling period. The output is observed and the process is repeated. Note that 4 predictions are made and 4 Js are evaluated during

every sampling period before an optimal control action, $U_{(k)}$, is selected for the next sampling period.

$$\min J_{(k+1)} = \sum_{k=1}^{k+N-1} (Y_{(k)} - r_{(k)}) \quad (19)$$

V. Simulation Results

To evaluate the effectiveness of the proposed SPI-MPC model, the model was connected to 3 kW PV array designed based on the findings of our previous study [21]. G and T were allowed to vary to generate different amount of PV power and MPC-SPI was used to inject the power into the grid at residential/distribution level of 120 V and 60 Hz. Table II lists the parameters for the simulation.

Fig. 8 shows $\alpha\beta$ (Vs and T/4 delayed Vs), dq voltages and theta for grid synchronization. Vα and Vβ are 90 degrees out of phase as expected due to T/4 delay. V_d regulated to zero and V_q equaled to V_s=170V. Theta goes from 0 to 2π radians and then resets to zero for another cycle due to mod(2π) function used in the implementation of PLL.

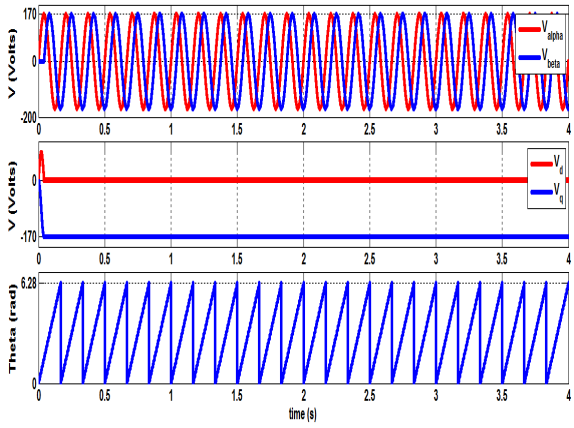

Fig. 8 $\alpha\beta$, dq voltages and theta

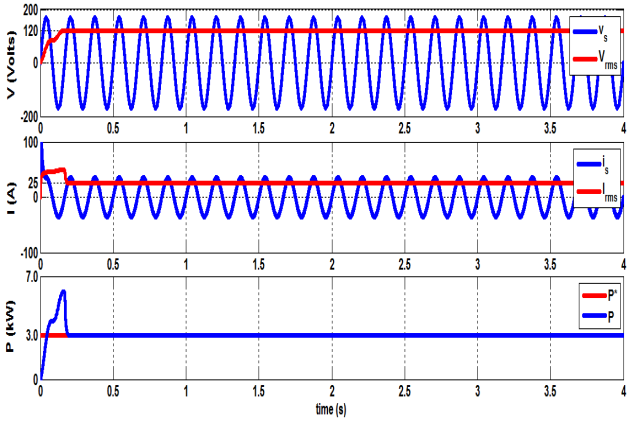

Fig. 9 V_s and i_s at fixed P

Fig. 9 shows Vs peaking at 170V with 120V rms. The current i_s is sinusoidal and peaks at approximately 35 amps with 25 amps rms. Since the power produced by the PV system remains fixed at 3kW, the value of i_s remains fixed too. Fig. 9 also shows SPI tracking reference power (P*).

Finally, Fig. 10 is the same as Fig. 9; however, it shows the behavior of the system with varying reference. G and T are allowed to change; therefore, the power produced by 3kW PV varies from its initial value of 1kW to 2kW at t=1.5s and from 2kW to 3kW at t=3s. Vs behaves as expected and i_s changes with PV system in steps (i.e., at 1.5s and 3s) to deliver the changing power into the grid.

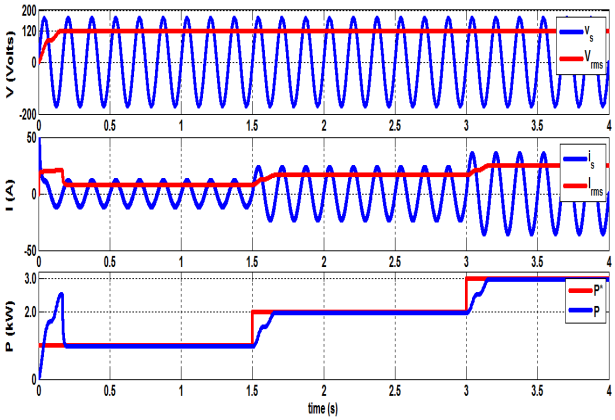

Fig. 10 V_s and i_s at varying P

VI. Conclusions

We presented the MPC of a UI-SPI for a PV system at residential/distribution level. MPC based UI-SPI model resulted in a simpler control and implementation without sacrificing quality and accuracy. The conventional PWM and PI regulators which can cause poor performance and saturation were avoided. The model was validated in Matlab/Simulink and the results showed the adequacy of the proposed model in tracking the reference.

TABLE II
Simulation Parameters

Parameter	Value
r	1 mΩ
L	500 µH
V_s	120 V
f_s	60 Hz
T_s	1 µS
PV system	3 kW
C_{DC}	660 uF
V_{DC}	300 V

References

[1] R. J. Wai, C. Y. Lin, Y. C. Huang, and Y. R. Chang, "Design of high-performance stand-alone and grid-connected inverter for distributed generation applications," IEEE Trans. Ind. Electron., vol. 60, no. 4, (2013).

[2] C. Trujillo, D. Velasco, G. Garcera, E. Figueres, and J. Guacaneme, "Reconfigurable control scheme for a PV micro-inverter working in both grid-connected and island modes," IEEE Trans. Ind. Electron., vol. 60, no. 4, (2013).

[3] M. Monfared, S. Golestan, and Josep M. Guerrero, "Analysis, Design, and Experimental Verification of a Synchronous Reference Frame Voltage Control for Single-Phase Inverters" IEEE Trans. Ind. Electron., vol. 61, no. 1, (2014).

[4] The world wind energy association "world wind energy report 2009"(http://www.wwindea.org/home/images/stories/worldwindenergyreport2009_s.pdf) (accessed February, 2014).
[5] The National Renewable Energy Lab report "2012 Renewable Energy Data Book" (http://www.nrel.gov/docs/fy14osti/60197.pdf) (accessed February, 2014).
[6] G. Paul, S. A. Kannan, N. Johnson, and J. George, "Modeling And Analysis of PV Micro-Inverter", International Journal Of Innovative Research In Electrical, Electronics, Instrumentation and Control Engg., Vol. 2, Issue 2, (2014).
[7] http://us.sunpowercorp.com/ (accessed May, 2014)
[8] http://www.advanced-energy.com/ (accessed June, 2014).
[9] http://www.sma-canada.ca/ (accessed June, 2014).
[10] K. Zhou, K. Low, D. Wang, F. Luo, B. Zhang, and Y. Wang, "Zero-phase odd-harmonic repetitive controller for a single-phase PWM inverter," IEEE Trans. Pow. Elec., vol. 21, no. 1, (2006).
[11] K. Zhang, Y. Kang, J. Xiong, and J. Chen, "Direct repetitive control of SPWM inverter for UPS purpose," IEEE Trans. Power Electron., vol. 18, no. 3, (2003).
[12] T. Fujii and T. Yokoyama, "FPGA based deadbeat control with disturbance compensator for single-phase PWM inverter," in Proc. IEEE Pow Elec. Spec. Conf., (2006).
[13] P. Mattavelli, "An improved deadbeat control for UPS using disturbance observers," IEEE Trans. Ind. Elec., vol. 52, no. 1, (2005).
[14] A. Abrishamifar, A. A. Ahmad, and M. Mohamadian, "Fixed switching frequency sliding mode control for single-phase unipolar inverters," IEEE Trans. Pow. Elec., vol. 27, no. 5, (2012).
[15] T. L. Tai and J. S. Chen, "UPS inverter design using discrete-time sliding mode control scheme," IEEE Trans. Ind. Electron., vol. 49, no. 1, (2002).
[16] M. Mosa, H. Abu-Rub, M. E. Ahmed, A. Kouzoul, J. Rodríguez, "Control of Single Phase Grid Connected Multilevel Inverter Using Model Predictive Control", 4th International Conference on Power Engineering, Energy and Electrical Drives Istanbul, Turkey, (2013).
[17] Y. Xue, L. Chang, S. B. Kjær, J. Bordonau, and T. Shimizu,"Topologies of Single-Phase Inverters for Small Distributed Power Generators: An Overview", IEEE Trans. Power Electron., vol. 19, no. 5, (2004).
[18] S. B. Kjaer, J. K. Pedersen, and F. Blaabjerg, "A Review of Single-Phase Grid-Connected Inverters for Photovoltaic Modules" IEEE Trans. Ind. Appl., vol. 41, no. 5, (2005).
[19] M. Morari and J. H. Lee, "Model predictive control: past, present and future," Computers and Chemical Engineering, vol. 23, (1999).
[20] J. Rodríguez, Pontt, C. Silva, P. Correa, P. Lezana, P. Cortés, U. Ammann, "Predictive current control of a voltage source inverter," IEEE Transactions on Industrial Electronics, vol. 54, no. 1, (2007).
[21] I. M. Syed and A. Yazdani, "Simple Mathematical Model of Photovoltaic Module for Simulation in Matlab/Simulink", Canadian Conference on Electrical and Computer Engineering, IEEE,(2014).